Evidence for subsurface Auger processes during interactions of N^{7+} ions with a Ni(110) target

J. Das, L. Folkerts, and R. Morgenstern
Kernfysisch Versneller Instituut, University of Groningen, Zernikelaan 25, 9747 AA Groningen, The Netherlands
(Received 1 November 1991)

We present secondary-electron spectra arising from collisions of N^{7+} ions with a Ni(110) target for kinetic energies ranging between 150 eV and 20 keV and also for different observation angles. The filling of the two K-shell holes in N^{7+} requires two consecutive KLL Auger processes, giving rise to a double structure in the KLL peak. The ratio of the intensities of the two KLL peaks depends on the collision energy as well as on the angle of observation. We show that this dependence can be explained by assuming that the KLL electrons are emitted after the projectile has penetrated the surface.

PACS number(s): 79.20.Nc, 34.90.+q

I. INTRODUCTION

The interaction of highly charged ions with metal surfaces has been extensively investigated in recent years [1–6]. The picture emerging from these investigations is one in which the ion is rapidly neutralized by electron capture from the surface. Previous studies [2–5] have suggested that this neutralization occurs while the projectile is still moving towards the surface. This picture is based on the fact that the K Auger and L Auger electrons emitted by the projectile ions show a Doppler shift for different observation angles. The shift is characteristic of electrons that are emitted from the moving projectile before it has undergone appreciable deviation from its initial trajectory. This fact has commonly resulted in the assumption that the Auger electrons are emitted before the projectile has penetrated the surface. However, a recent study [7] shows that the observation of a Doppler shift in the electron-energy spectra is not sufficient to prove that the electrons are emitted above the target surface. Meyer *et al.* [7] have measured the K Auger electron emission during collisions of N^{6+} on Au(110) and they find that the emitted electrons come predominantly from beneath the surface although the electron spectra show a Doppler shift corresponding to the initial trajectory of the projectile. Their conclusion is that the electrons are emitted by the projectile after it has penetrated the surface but before its trajectory has changed.

To further investigate the *subsurface emission* of Auger electrons we have measured the electron spectra emitted during collisions of N^{7+} on a Ni(110) surface for different projectile energies and observation angles. The kinetic energy of the projectiles ranged between 150 and 20 keV and the detection angle was varied between 60° and 135°. In the present paper we show that the intensity of measured KLL electron spectra provides definitive evidence that these electrons are indeed emitted after the projectile has penetrated the surface.

II. EXPERIMENTAL METHOD

The measurements were carried out in a ultrahigh-vacuum (UHV) μ-metal collision chamber with a Ni(110) target sputter cleaned by Ar ions. The base pressure of the collision chamber was below 2×10^{-8} Pa. Beams of N^{6+} and N^{7+} ions were produced by the KVI-ECR ion source [8] at energies of 62 and 84 keV, respectively. The ion beams were then transported to the experimental setup and decelerated to the collision energy by floating the complete apparatus on a positive voltage. The electron spectra were measured with a 180° spherical electrostatic analyzer equipped with a channeltron, which can be rotated over a large range of detection angles. The energy resolution of the analyzer is $5 \times 10^{-3}E$ full width at half maximum (FWHM) and its acceptance at the center of the target is $11.2 \times 10^{-8}E(\mathrm{sr\,eV})$, with E being the energy of the detected electrons in eV. Due to residual magnetic fields the lowest energy at which electrons can be measured reliably is $\approx$ 25 eV. A more detailed description of the apparatus is presented elsewhere [2].

III. ELECTRON-ENERGY SPECTRA

Figure 1 shows the electron spectra measured for 150 eV N^{q+} ($q = 6,7$) ions colliding with a Ni(110) target. Definite peak structures are present at both the high- and low-energy side of the spectra. The structure at the low-energy side is due to LMM Auger electrons, as has been previously reported [4]. The high-energy peaks are the result of KLL Auger electrons. Comparing the spectra it can be seen that both the KLL and LMM peaks in N^{7+} show a double structure that arises due to the presence of two K-shell holes in N^{7+} [9]. The LMM electrons that are emitted when the two K-shell holes are still present in the projectile are higher in energy compared to those emitted when one K hole has been filled due to screening of the core charge by the first captured K electron. This results in the double LMM peak in the N^{7+} spectrum.

The filling of the two K-shell holes requires two consecutive K Auger processes and the two KLL peaks are thus ascribed to the K_0LL and K_1LL processes where the subscript denotes the number of K-shell electrons in the initial state. As in the case of the LMM electrons, the K_1LL electrons are lower in energy compared to the K_0LL electrons because of the core screening by the first K electron. N^{6+} has a single K-shell hole which is reflected in the fact that neither the KLL nor the LMM peaks in N^{6+} show the double structure associated with N^{7+}. Figure 2 shows the electron spectra arising from the collision of 500-eV N^{6+} and N^{7+} on Ni. The high-energy shoulders of the KLL peaks are ascribed to KLX Auger electrons. At even higher energies one finds evidence of the higher series KMX and KNX. As expected, the intensities of the electrons arising from the higher Auger series are very small compared to the KLL intensities.

The KLL electrons are ascribed to emission from the moving projectile and should therefore contain information about the motion and the electronic environment of these projectiles at the moment of electron emission. We have measured the Doppler shifts of the electron energies to determine the emitter velocity. We have also measured the ratio of the K_0LL and K_1LL intensities as a function of the collision velocity and as a function of the electron emission angle. The latter two measurements are based on the consideration that the double KLL peak in the N^{7+} spectrum can be used to determine the point of origin of the KLL electrons. If these electrons are indeed due to *subsurface emission*, from incoming projectiles, then the K_1LL electrons are on average emitted from a greater depth inside the target as compared to the K_0LL electrons. This results from the fact that for a specific ion the K_0LL process always precedes the K_1LL process in time. The escape probability of the Auger electrons from the target depends on the depth where they are emitted and on the emission angle with respect to the surface normal. This dependence on the depth and emission angle can be directly correlated to a dependence on the kinetic energy of the projectile and on the angle of observation. Therefore, the ratio of the intensities of the K_1LL and K_0LL peaks should also demonstrate a dependence on the projectile kinetic energy and the detection angle.

The results of the Doppler-shift measurements are presented in Fig. 3. They show the position of the half-maximum point of the high-energy side of the K_0LL peak as a function of the detection angle for two different projectile energies. The solid curve is a calculation of the Doppler shift assuming that the decay occurs while the projectile is still in its initial trajectory while the dashed curve is a least-squares fit to the measured data with the energy of the projectile as a free parameter. The energies resulting from these fits are 1.2 and 3.6 keV for the 2- and 10-keV measurements, respectively. The discrepancy between these two curves clearly indicates that the velocity of the projectile has changed prior to the emission process—presumably as a consequence of the projectile's interaction with the solid. This effect seems to be more pronounced at higher incident energies.

Before entering into a more detailed discussion of this effect we present the results of measurements performed to study the intensity ratio of the K_0LL and K_1LL peaks. We have determined this intensity ratio for electrons resulting from the impact of N^{7+} on Ni for collision energies ranging from 150 eV to 20 keV and also for different detection angles. In order to calculate the functional form of the dependence of the intensity ratio on the collision energy and detection angle we do the following. We as-

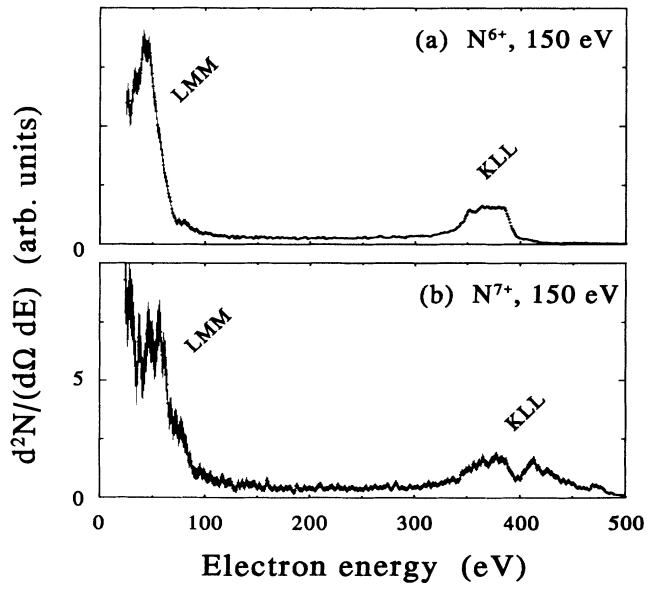

FIG. 1. Secondary-electron energy spectra arising from collisions of 150-eV N^{q+} ($q = 6, 7$) with Ni(110).

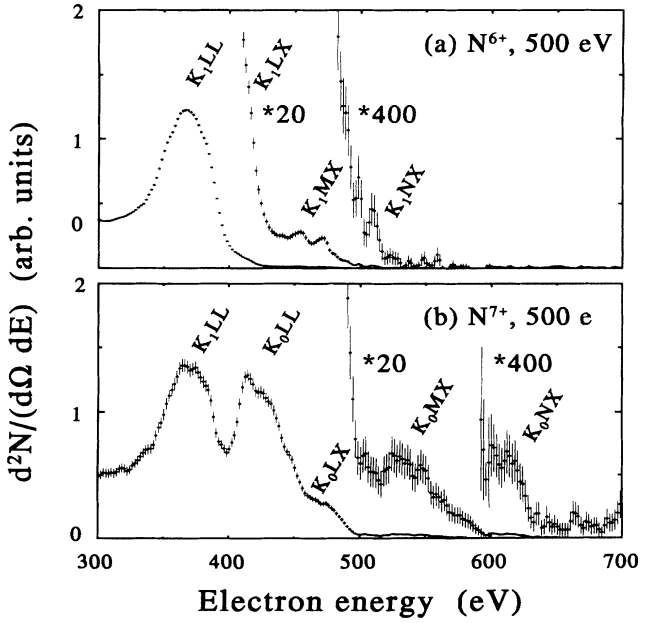

FIG. 2. Secondary-electron energy spectra arising from collisions of 500-eV N^{q+} ($q = 6, 7$) with Ni(110) where the high-energy part of the spectrum has been magnified to show the contribution of electrons from the higher Auger series.

sume that the neutralization of the projectile proceeds via multiple electron capture into the outer shells and that there is no direct capture into the K shell. Experiments [4, 6, 10, 11] have shown that the projectile outer shells are completely neutralized prior to K Auger decay, proving the validity of this assumption. The filling of the K shell is described in terms of three states—the initial state with two K-shell holes, the intermediate state with one K-shell hole, and finally the state where the K shell is completely filled. The population numbers of these states, respectively n_0, n_1, and n_2, are determined by the transition rates between them. The following set of coupled differential equations has to be solved to determine the time evolution of the population numbers:

$$\frac{dn_0}{dt} = -\Gamma_0 n_0, \tag{1a}$$

$$\frac{dn_1}{dt} = \Gamma_0 n_0 - \Gamma_1 n_1, \tag{1b}$$

$$\frac{dn_2}{dt} = \Gamma_1 n_1, \tag{1c}$$

where Γ_0 and Γ_1 are the Auger transition rates of the K_0LL and K_1LL processes, respectively. At any given time t the population numbers are

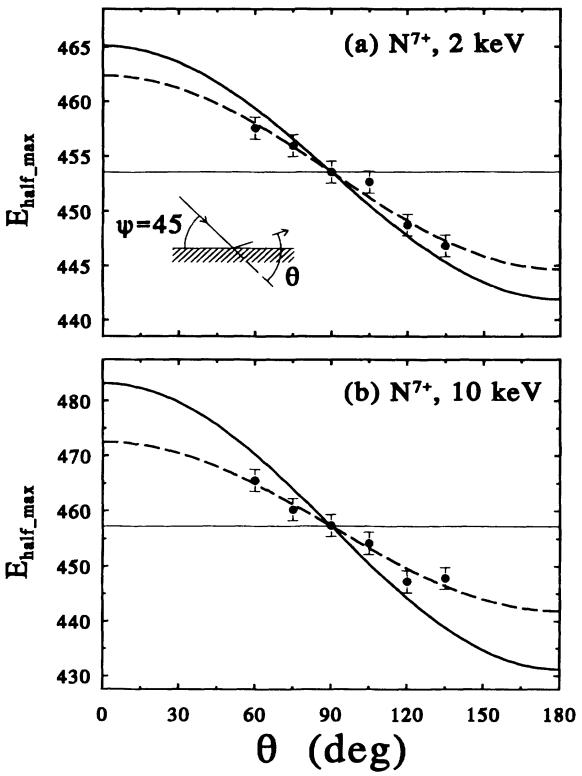

FIG. 3. Position of the high-energy side at half maximum of the K_0LL peak for 2- and 10-keV $N^{7+} \rightarrow$ Ni(110) as a function of the detection angle θ. The solid curve is a calculation of the Doppler shift, assuming that the decay occurs while the projectile is still in its initial trajectory, while the dashed curve is a least-squares fit to the measured data with the energy of the projectile as a free parameter.

$$n_0(t) = Ne^{-\Gamma_0 t}, \tag{2a}$$

$$n_1(t) = N\frac{\Gamma_0}{\Gamma_1 - \Gamma_0}\left(e^{-\Gamma_1 t} - e^{-\Gamma_0 t}\right), \tag{2b}$$

$$n_2(t) = N\left(1 + \frac{\Gamma_1}{\Gamma_0 - \Gamma_1}e^{-\Gamma_0 t} - \frac{\Gamma_0}{\Gamma_0 - \Gamma_1}e^{-\Gamma_1 t}\right), \tag{2c}$$

where N is the normalization factor. The escape probability of an electron emitted inside a solid in a specified direction is given by

$$P(d,\eta) = \exp\left(-\frac{d}{\lambda\cos\eta}\right), \tag{3}$$

where d is the depth below the surface, λ the inelastic mean free path of the Auger electrons, and η the angle of observation relative to the surface normal. We assume for simplicity that the projectile does not undergo appreciable angular scattering in the bulk before emission of the K Auger electrons. Monte Carlo simulations of projectile trajectories inside the target by Meyer *et al.* [7] show that very little angular scattering occurs over depths comparable to the inelastic mean free paths of the Auger electrons. Equation (3) can then be written in terms of the perpendicular velocity $v_\perp$ of the projectile as

$$P(t,\theta) = \exp\left(-\frac{v_\perp t}{\lambda\sin(\theta - \psi)}\right). \tag{4}$$

Here t is the time taken by the projectile to penetrate a depth d, ψ the angle of incidence on the surface, and θ the detection angle with respect to the projectile direction (see Fig. 4).

The fraction of electrons, emitted by each KLL process that is observed at an angle θ is thus given by

$$I_{K_0LL} = \int_0^\infty \frac{dn_0(t)}{dt}P(t,\theta)dt, \tag{5a}$$

$$I_{K_1LL} = \int_0^\infty \frac{dn_2(t)}{dt}P(t,\theta)dt. \tag{5b}$$

The ratio R of the intensities of the K_1LL and K_0LL processes can then be written as

$$R = \frac{I_{K_1LL}}{I_{K_0LL}} = \left(1 + \frac{v_\perp}{\Gamma_1\lambda\sin(\theta - \psi)}\right)^{-1}. \tag{6}$$

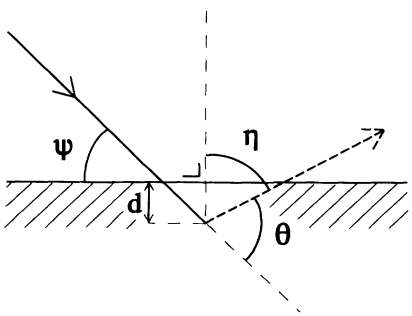

FIG. 4. Schematic of the experimental configuration showing the different angles.

From Eq. (6) it can be seen that the ratio R is independent of the transition probability Γ_0 of the K_0LL process. This result is not unexpected since the ratio depends only on the extra distance traversed by the projectile between the K_0LL and K_1LL processes. This distance is determined by the time between the two processes and hence on the transition probability of the second KLL process. The ratio depends on the probability that the K_1LL process happens fast enough for the electrons to reach the detector without being inelastically scattered in the target. This leads directly to a dependence on the velocity of the projectile. At velocities that are very low compared to $\Gamma_1\lambda$, the ratio approaches unity. As the energy of the projectile is increased $v_\perp$ becomes larger than $\Gamma_1\lambda$ and the value of R decreases.

In order to extract the K Auger electron yields from the measured spectra background, subtraction is done following the algorithm outlined in Refs. [12, 13]. The algorithm is based on the assumption that the electron signal at each energy contributes a uniform background to all points at lower kinetic energies. This provides a reasonable estimate of the background if the Auger peak is well defined relative to the low-energy continuum. Once the background has been subtracted the next step is the deconvolution of the double KLL peak into a part arising from the K_0LL process and another from the K_1LL process. We have used the following procedure to determine the individual contributions of the different processes. For each projectile energy we have measured the electron-energy spectra for both N^{6+} and N^{7+} ions. The N^{6+} spectrum has only the K_1LL peak, and the shape of this peak is then used to deconvolute the double KLL peak in the N^{7+} spectra. The underlying assumption in the above method is that the low-energy tail of the K_0LL peak has the same shape as that of the K_1LL peak. During the deconvolution correct normalization is achieved by requiring the sum of the deconvoluted spectra to be exactly equal to the original spectrum, at each energy channel. Figure 5 shows the background subtracted K Auger spectra for N^{6+} and N^{7+} ions colliding with a Ni(110) target. The final deconvoluted spectra are shown in the same figure. The intensity of the individual peaks is then calculated by integrating the spectra.

Figure 6 shows the ratio R of the two KLL peaks as a function of the projectile energy and Fig. 8 shows the same ratio as a function of the detection angle θ for two different projectile energies. It should be noted that the error bars indicated on the data points include only the statistical errors. Systematic errors arising from the choice of deconvolution procedure are estimated to be $\lesssim 10\%$. The curves drawn through the data points in both figures are the result of a fit to the data using Eq. (6). The only free parameter in the fit is the factor $\Gamma_1\lambda$.

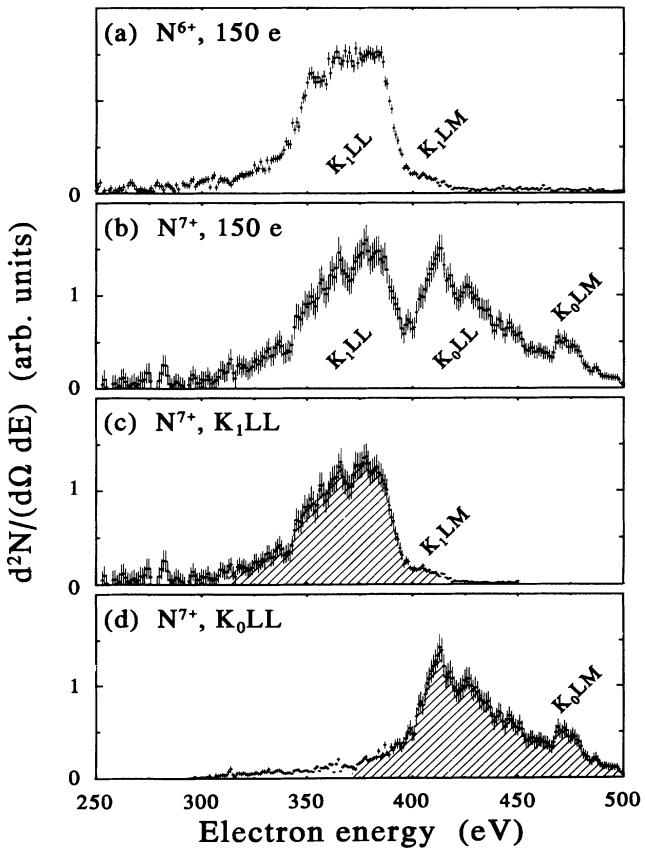

FIG. 5. Background-subtracted K Auger spectra for 150-eV N^{q+} ($q = 6, 7$) incident on Ni(110). The hatched areas indicate the regions over which the KLL peaks are integrated in order to calculate the intensity ratio I_{K_1LL}/I_{K_0LL}.

IV. DISCUSSION

It is evident from Figs. 6 and 8 that there is reasonable agreement between the experimental results and the calculations. Especially important is the angular dependence of the ratio as shown in Figs. 7 and 8. This angular dependence cannot be explained in terms of K Auger processes that take place above the surface. If the electrons are emitted prior to the penetration of the surface the

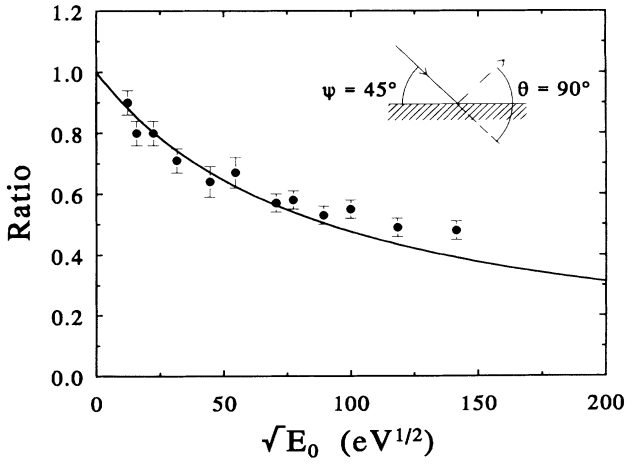

FIG. 6. The ratio R of the intensities of the K_1LL and K_0LL peaks as a function of the collision energy. The curve through the data points is the result of a fit using Eq. (6) with $\Gamma_1\lambda$ as the free parameter.

ratio would remain constant with a change in detection angle, provided that the K_0LL and K_1LL electrons have similar angular distributions. From Fig. 8 it can be seen that the change in R from its nominal value is most pronounced at small values of θ. However, at these values not only does the ratio R decrease rapidly but the complete KLL peak structure is also washed out, making it difficult to separate the individual components. From the fit to the experimental data the value of the fit parameter $\Gamma_1\lambda$ is found to be 3.4×10^5 m/s. Assuming a value of $\lambda = 10$ Å for the mean free path [14], the K_1LL transition probability Γ_1 turns out to be 3.4×10^{14} s^{-1}, a number that is in agreement with typical K Auger transition probabilities.

Subsurface emission of K Auger electrons can also be used to explain the velocity dependence of the K_1LL peak in hydrogenlike ions. It is seen that the intensity of the K_1LL peak decreases with increasing projectile energy. The most common explanation for this phenomenon is based on the assumption that at high kinetic energies the projectile does not have enough time to undergo the K_1LL process before reaching the target surface. Then the question still remains as to what happens to the projectile after it reaches the surface. But if the K_1LL electrons are emitted from beneath the target surface their escape probability is directly dependent on the distance they have to travel within the target before reaching the detector. The K_1LL electrons emitted by projectiles with high kinetic energies come on average from greater depths under the surface and have lower escape probabilities. Consequently the intensity of the K_1LL peak decreases with increasing energy of the projectile.

A further evidence in support of subsurface emission of Auger electrons is the fact that the autoionization cascade picture, commonly used to describe the neutralization dynamics of highly charged ions near metal surfaces, is inconsistent with experimental results. The autoionization cascade requires time scales that are long compared to K Auger lifetimes and is not consistent with experiments, which indicate a rapid and complete neutralization of the projectile outer shells prior to K Auger decay [4,6,10,11]. As pointed out in [7] this inconsistency can be removed if the K Auger electrons are assumed to be predominantly due to subsurface emission.

Although the experiments reported here definitely indicate that the K Auger electrons are emitted after the projectile has penetrated the target, it is not clear whether the projectile undergoes a change in trajectory prior to electron emission. The Doppler-shift measurements could possibly provide more information on this question. In our calculations shown in Fig. 3 we have assumed that the projectile does not undergo appreciable angular scattering prior to electron emission, but this may not be strictly true. Although the comparison of measurements and calculations indicate that the velocity of the projectile is different from its initial value, this does not necessarily imply that the projectile energy has changed. A similar result would be obtained if the projectile changed its trajectory rather than its energy. Köhrbrück *et al.* [15] have in fact reported that Doppler-shift measurements indicate that the K Auger electrons resulting from Ne^{9+} collisions are emitted from projectiles after they have been reflected off the target surface. However, we find that these results can as well be explained by assuming that the electrons are emitted by the incident projectile after it has experienced a slowing down of its velocity. Moreover a specular reflection of the projectiles, as is assumed by Köhrbrück *et al.*, certainly

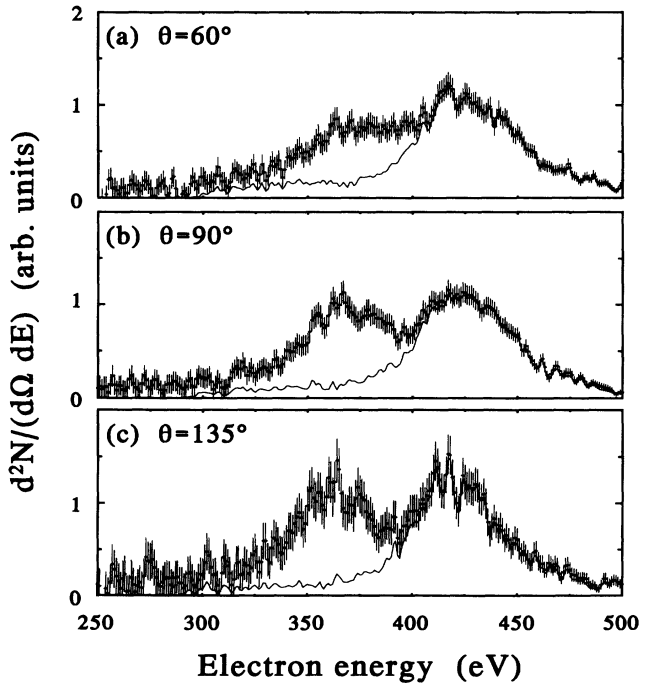

FIG. 7. Background-subtracted K Auger spectra for 2-keV N^{7+} incident on Ni(110) for different detection angles. The solid curve indicates the deconvoluted K_0LL peak.

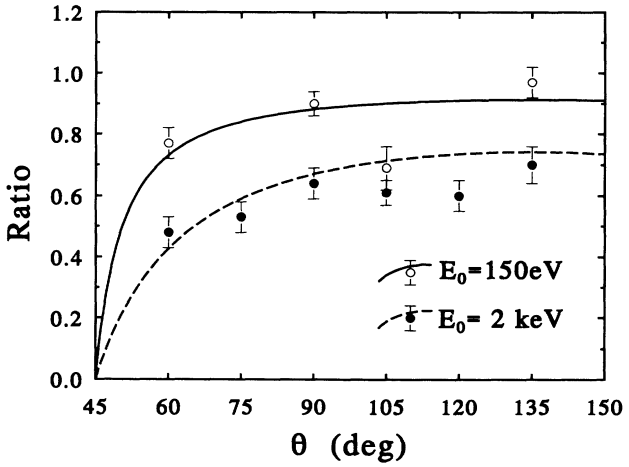

FIG. 8. The ratio R of the intensities of the K_1LL and K_0LL peaks as a function of the detection angle θ. Both curves through the data points are the result of a fit using Eq. (6) with $\Gamma_1\lambda$ as the free parameter.

does not take place at our experimental condition (angle of incidence 45°). Considering the simplest case, where the projectile is scattered symmetrically around its incident direction, it is evident that the Doppler shift measures the component of the average projectile velocity in the scattered direction rather than its full velocity. A decrease of this component as suggested by Fig. 3 could arise from an increase in the average scattering angle as well as from a decrease in the energy. As mentioned earlier, Monte Carlo simulations performed by Meyer *et al.* [7] of projectile trajectories inside the target show very little angular scattering over depths comparable with the inelastic mean free path of the Auger electrons. However, those trajectories that lead to electron capture in the L shell—and thus to KLL Auger processes—correspond to small-impact parameters and thus to larger than average scattering angles.

Finally we would like to point out that the results shown in Fig. 6 also give an indication that the projectiles have suffered an energy loss before the electron emission process: it can be seen that the agreement between the experimental and calculated curves becomes worse at higher incident energies. The discrepancies could be removed with the assumption that the high-energy projectiles suffer an appreciable energy loss before the electron emission process, as is also suggested by the Doppler-shift measurements.

V. CONCLUSION

We have measured the Auger-electron emission during interactions of N^{7+} ions with a Ni(110) target. The KLL Auger peak shows a double structure that is attributed to the two consecutive KLL processes required to fill the double K-shell hole in N^{7+}. The ratio of the intensities of the two KLL peaks depends on the kinetic energy of the projectile as well as on the observation angle. Calculations based on the assumption that the K Auger electrons are due to subsurface emission were able to reproduce the general trends shown by the experimental results very well. We find that the measurement of the angular dependence of the intensity ratio of the two KLL peaks provides an unambiguous way of determining the point of origin of the K Auger electrons. This holds true for all Auger electrons, provided one can measure the intensities of two consecutive Auger processes. Using the ratio of the intensities rather than the absolute intensities removes errors arising from normalization procedures.

It should, however, be noted that in our calculations we have only considered electrons that are emitted from beneath the target surface. A more exact treatment will have to include contributions from electrons that are emitted prior to the projectile penetrating the surface. This is especially true for very low projectile energies where the interaction time above the surface is very long [7].

ACKNOWLEDGMENTS

We would like to thank J. Eilander, R. Kremers, and J. Sijbring for their excellent technical support. This work is part of the research program of the Stichting voor Fundamenteel Onderzoek der Materie (FOM) with financial support from the Nederlandse Organisatie voor Wetenschappelijk Onderzoek (NWO).

[1] K. J. Snowdon, C. C. Havener, F. W. Meyer, S. H. Overbury, and D. M. Zehner, Phys. Rev. A **38**, 2294 (1988).
[2] S. T. De Zwart, A. G. Drentje, A. L. Boers, and R. Morgenstern, Surf. Sci. **217**, 298 (1989).
[3] F. W. Meyer, C. C. Havener, S. H. Overbury, K. J. Reed, K. J. Snowdon, and D. M. Zehner, J. Phys. (Paris) Colloq. **50**, C1 (1989).
[4] L. Folkerts and R. Morgenstern, Europhys. Lett. **13**, 373 (1990).
[5] J. P. Briand, L. de Billy, P. Charles, S. Esaabaa, P. Briand, R. Geller, J. P. Declaux, S. Bliman, and C. Ristori, Phys. Rev. Lett. **65**, 159 (1990).
[6] P. A. Zeijlmans van Emmichoven, C. C. Havener, and F. W. Meyer, Phys. Rev. A **43**, 1405 (1991).
[7] F. W. Meyer, S. H. Overbury, C. C. Havener, P. A. Zeijlmans van Emmichoven, and D. M. Zehner, Phys. Rev. Lett. **67**, 723 (1991).
[8] A. G. Drentje and J. Sijbring, in Oak Ridge National Laboratory Report No. Conf. 9011136 (unpublished), p. 17.
[9] P. Moretto-Capelle, A. Bordenave-Montesquieu, P. Benoit-Cattin, S. Andriamonje, and H. J. Andrä, Suppl. Z. Phys. D **21**, S347 (1991).
[10] L. Folkerts and R. Morgenstern, Suppl. Z. Phys. D **21**, S351 (1991).
[11] H. J. Andrä, Nucl. Instrum. Methods B **43**, 306 (1989).
[12] D. A. Shirley, Phys. Rev. B **5**, 4709 (1972).
[13] H. E. Bishop, Surf. Interf. Anal. **3**, 272 (1981).
[14] L. C. Feldman and J. W. Mayer, *Fundamentals of Surface and Thin Film Analysis* (Elsevier Science, New York, 1986), p. 129.
[15] R. Köhrbrück, D. Lecler, F. Fremont, P. Roncin, K. Sommer, T. J. M. Zouros, J. Bleck-Neuhaus, and N. Stolterfoht, Nucl. Instrum. Methods B **56/57**, 219 (1991).